A novel valveless pulsatile flow pump for extracorporeal blood circulation

Joaquín Anatol* [1], Emanuele Vignali [2], Emanuele Gasparotti [2], Francisco Castro-Ruiz [1], Manuel Rubio [1], César Barrios-Collado [1], Jose Sierra-Pallares [1], and Simona Celi [2]

[1]*Departamento de Ingeniería Energética y Fluidomecánica, Universidad de Valladolid, Paseo del Cauce 59, 47011 Valladolid, Spain*

[2]*BioCardioLab, Fondazione Toscana G. Monasterio, Massa 54100, Italy*

*Correspondence author: joaquin.anatol@uva.es

Key words: extracorporeal blood circulation, mock circulatory loop, valveless pumping.

Abstract

Extracorporeal Membrane Oxygenation (ECMO) is a modality of extracorporeal life support which allows temporary support in cases of cardiopulmonary failure and cardiogenic shock. This study presents a valveless pump that works by the Liebau effect as a possible pumping system in ECMO circuits, replacing the current roller and centrifugal pumps. For this purpose, a mock circulatory loop emulating the haemodynamic of the right part of the heart has been constructed. A veno-venous ECMO circuit (VV-ECMO) with the integrated Liebau pump has been incorporated to analyse its performance. The Liebau pump in the ECMO circuit showed a flow assistance in the range of paediatric ECMO and low blood flow range for adults. In addition, Experimental test conducted demonstrated the advantage of the Liebau pump over currently used pumps as the ability to generate a pulsatile flow, which has many advantages in biomedical applications.

Introduction

Extracorporeal membrane oxygenation (ECMO) is artificial extracorporeal procedure to support the respiratory and/or cardiac system adopted in case of cardiopulmonary failure and cardiogenic shock [1–6]. This methodology has been around since the 1970s [7,8] and although initially there were many complications in its

applicability, technological advances related to ECMO mean that currently its benefits outweigh its risks [9–12]. Thus, the use of ECMO in patients with cardiopulmonary diseases has increased in recent times [13–15]. By 2020 the Extracorporeal Life Support Organization (ELSO) had recorded >24,000 cases of adult respiratory ECMO [16]. Nowadays several studies are devoted to the investigation of ECMO behaviour by adopting engineering approaches [17–19].

Two separate configurations of ECMO exists: veno-venous (VV) and veno-arterial (VA). Both types involve the blood draining from venous system to the extracorporeal circuit and the oxygenated blood supplying to the circulation. In cases of respiratory failure where cardiac function is preserved, the veno-venous configuration (VV-ECMO) is used. On the other hand, when cardiac support is required, the veno-arterial configuration (VA-ECMO) is used whether lung function is preserved or not [20]. Due to a better oxygenation quality, VV-ECMO often improves cardiac function despite the absence of direct arterial support [21,22]. In most cases in the VV-ECMO configuration, blood leaves the right atrium through the inferior vena cava into the ECMO circuit via a femoral venous access. Blood returns to the right atrium via the superior vena cava through an internal jugular venous access.

The standard ECMO circuit is composed of the following main elements: a pump, drainage and return cannulae, lines and an oxygenator. Concerning the pumping system, roller pumps have been used for decades, but have been replaced by centrifugal pumps [23–25]. The technical advances in centrifugal pumps have succeeded in reducing the risk of thrombosis and haemolysis on ECMO circuits [26]. On the other hand, the non-pulsatile flow generated by centrifugal pumps leads to acute kidney injury, especially in neonates [10]. In fact, it was reported that a pulsatile flow plays a key role to ensure and to maintain an efficient circulatory flow for a better end-organ function [27] and to reduce neurological complications [28].

The ELSO registry that included all reported ECMO runs for patients aged 18 years or younger between 2010 and 2015 concluded that haemolysis and kidney injury were complications reported when using centrifugal pumps in 14% and 20% of cases, respectively [29]. A recent study [30] concluded that 45% of centrifugal pumps tested in ECMO circuits had thrombus formation in the pump impeller. In [31], it was found a 41% incidence of thrombus in centrifugal pumps. Another problem is the recirculation of

already oxygenated blood to the ECMO system due to the absence of pulsatility of centrifugal pumps [32–34].

To overcome the current issues of ECMO actuation systems, it might be interesting to explore different pumping technologies. An example is given by the Liebau pump. The performance of the proposed pump and its principle of operation, the Liebau effect [35], have been extensively reviewed in previous works [36–42].

Liebau pump can generate a pulsatile flow without the use of mechanical valves by periodic pinching of a compliant tube, attached at its ends to a stiffer tube, and with an asymmetry: either in the pincher location or in the circuit configuration or both simultaneously [43–47]. In addition, it has no mechanical elements in contact with the fluid that could damage the blood cells. Concerning the pincher, soft robotics technology has recently been used. It has some advantages over other possible pinchers, such as a smaller size, biocompatibility, and increased durability of the compliant tube [42]. Its characteristics and mode of operation have been presented in previous works [41]. Based on the aforementioned consideration, the adoption of a Liebau pump seems a promising approach as an alternative to classic ECMO pumping systems.

The aim of this work is to evaluate the feasibility of a valveless Liebau pump for ECMO. For this purpose, a VV-ECMO circuit with a Liebau pump was developed and integrated with a mock circulatory loop replicating the right heart morphology and circulation. The Liebau pump was tested without the physiological cycle to analyse its behaviour. Subsequently, with the physiological cycle present, its performance has been tested in terms of net pumped flow and instantaneous flow profiles for different operating parameters and pinching frequencies.

Materials and methods

Experimental test rig

The test rig reproduces the circulatory loop in the right atrium of the heart where physiological flow evolution present in the venae cavae and tricuspid valve has been emulated. The test rig consists of two circuits: the Right Atrium Mock Circulatory Loop (RA-MCL) and the VV-ECMO circuit with Liebau Pump (VV-LP). The experimental setup is shown in Figure 6.1. Water was used as the working fluid.

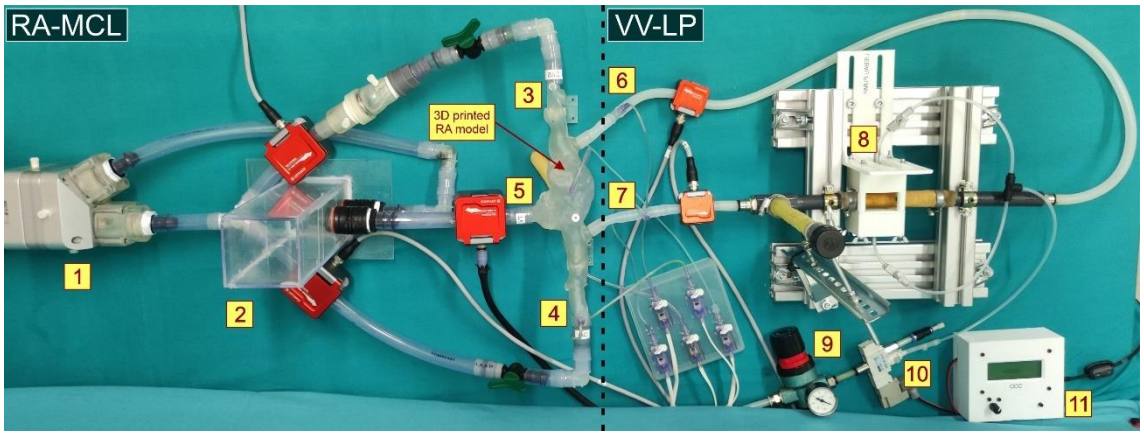

Figure 6.1. Experimental test rig indicating the RA-MCL circuit with the 3D anatomical model and the VV-LP circuit. (1) Piston pump, (2) reservoir, (3) superior vena cava, (4) inferior vena cava, (5) tricuspid valve orifice, (6) return line, (7) drainage line, (8) Liebau pump module, (9) pressure regulator, (10) electrovalve and (11) Operating Cycle Control module.

RA-MCL circuit - The Mock Circulatory Loop consists of a 3D anatomical model and both passive and active hydraulic elements. The 3D anatomical model is a printed model of the right atrium (RA) including the tricuspid valve (TV) orifice, the inferior vena cava (IVC) and the superior vena cava (SVC). The passive components include: a reservoir, a tubing assembly (flexible PVC, 18 mm inner diameter) to connect the system elements and regulating valves to control the flow through the circuit. A specific check-valve has been incorporated in the superior vena cava branch to avoid reverse flow recirculation between the two venae cavae. The circuit is activated by a piston pump (PP).

The anatomical model was fabricated starting from the segmentation of a CT-dataset and using additive manufacturing technique [Figure 6.2a]. Stereolithographic technique was adopted using a 3BL Form printer machine (Formlabs, USA) and the commercial Clear Resin was used to obtain a rigid and transparent model [48]. The 3D printed model was designed with five connectors for its coupling with the rest of the rig, three *luer* taps to measure the pressure at different sites of the model and an orifice to vent air [Figure 6.2b-c]. Additionally, specific supports were included to allow the model orientation. Due to the rigidity of the model, a compliant chamber (CC_{RA}) has been incorporated to reproduce the compliance of the atrium during the physiological cycle. The CC_{RA} consists of a latex tube with a thickness of 0.3 mm, an internal diameter of 20 mm and an adjustable length L_{CCRA} [Figure 6.2c].

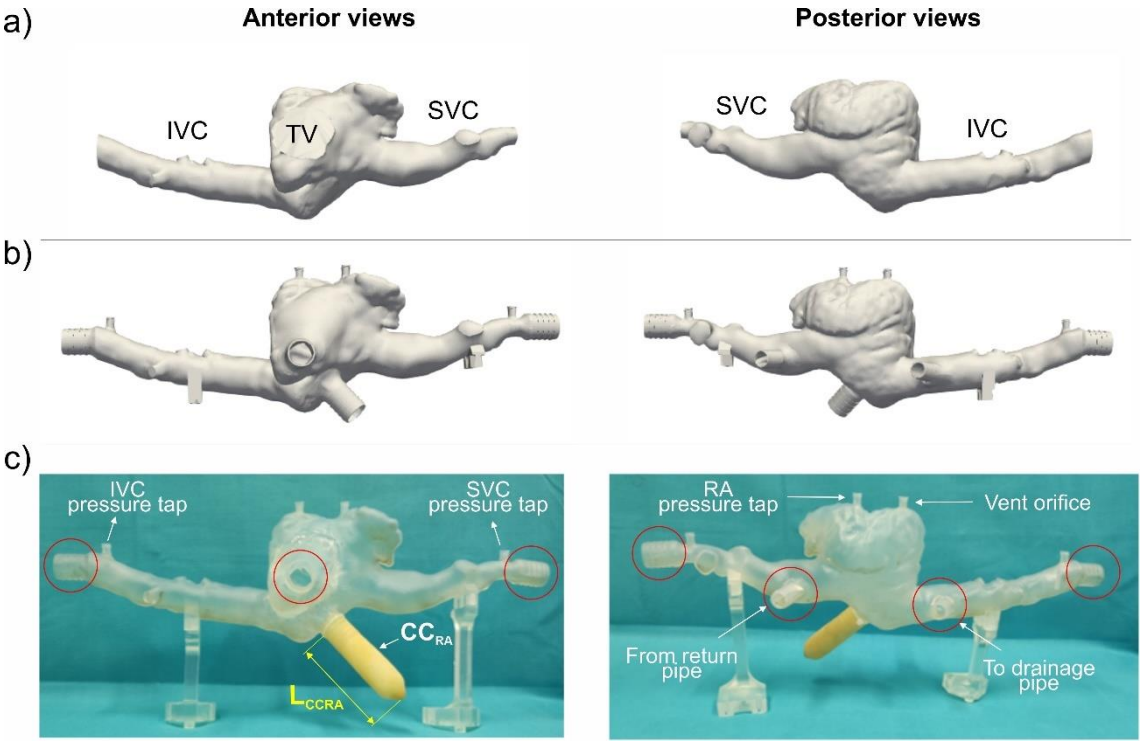

Figure 6.2. Anterior and posterior views of: (a) 3D segmented model; (b) 3D anatomical model with connections and (c) 3D printed model with the CC_{RA}, pressure taps, vent orifice, and connectors (red circles).

The anatomical model is connected to a reservoir through the TV orifice and to the piston pump through the venae cavae. The piston pump delivers fluid from the reservoir into the right atrium via the venae cavae. The piston system pumps the flow to the anatomical model by imposing a parameterised flowrate temporal profile [49,50].

VV-LP circuit - The VV-ECMO circuit with Liebau Pump consists of a Liebau pump module (LPM) connected to the 3D model via a drainage and a return line [Figure 6.3]. The drainage and return lines had a flexible part made of Platinum-Cured Silicone and a rigid part made of PVC. Drainage line and return line had a length of L_D and L_R, respectively. The position of the associated connectors in the 3D model are at the junction of the venae cavae with the right atrium, according to a double cannulation configuration [51].

The Liebau pump module consists of a pincher that compresses a compliant tube [Figure 6.3b] to generate the pumping phenomenon, a compliant chamber (CC) and two rigid pipes of polyvinyl chloride (PVC). The rigid pipe 1 houses the compliant chamber which reduces flow fluctuations in the drainage line and eliminates reverse flow [41] into the atrium [Figure 6.3]. The rigid pipes are joined by the latex compliant tube. The pincher

is a soft robot, pneumatically driven by compressed air at an operating pressure, P_t. It is placed inside a rigid housing which forces it to deform only towards the compliant tube, compressing it, [Figure 6.3b].

The configuration of the LPM assumes an asymmetric position of the pincher in the compliant tube towards the drainage line side and an asymmetry in the circuit at the ends of the compliant tube. In previous works [41] this configuration had best overall performance.

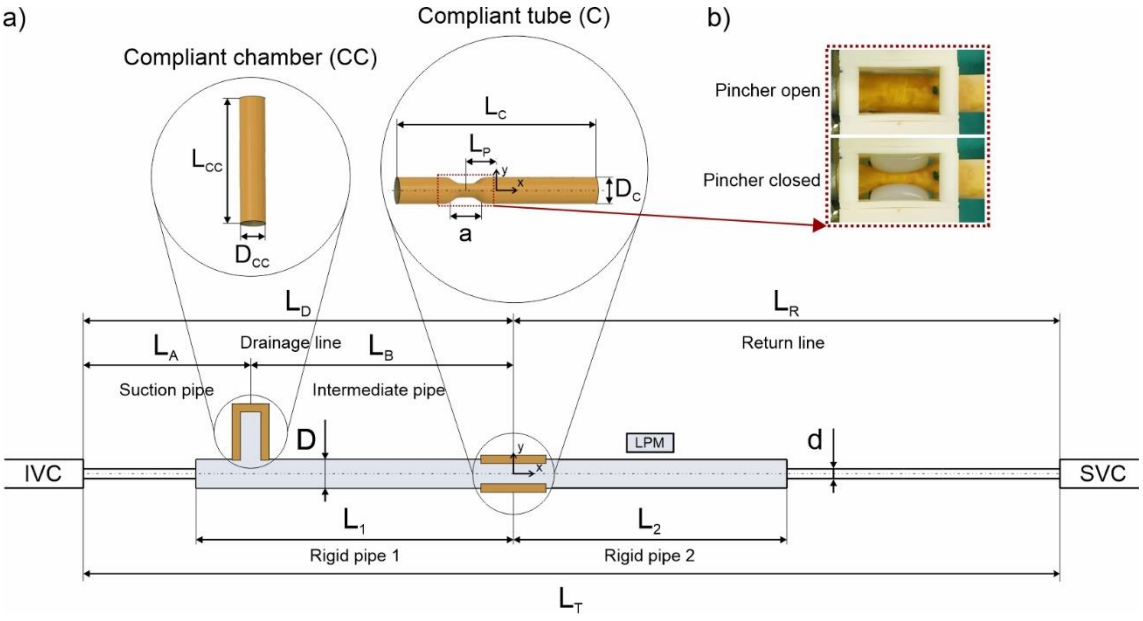

Figure 6.3. (a) Schematic of the VV-LP circuit with the LPM. (b) Detail of the pincher and the compliant tube

The components of the VV-ECMO circuit with Liebau Pump have the dimensions shown in the schematic in Figure 6.3. The baseline values of these geometrical parameters are shown in Table 6.1. The length of a commercial VV-ECMO circuit is around 200 cm in length, therefore, L_T= 200 cm was set as the baseline value. The length ratio is defined as $\lambda_M = L_R/L_B$.

Table 6.1. Baseline values of the VV-LP circuit parameters

Parameter	**D**	**d**	**L_1**	**L_2**	**L_A**	**L_B**
Value	16 mm	10 mm	22 cm	21 cm	39 cm	17 cm

Parameter	L_D	L_R	L_T	D_C	wt_C	L_C
Value	56 cm	144 cm	200 cm	20 mm	0.7 mm	10 cm

Parameter	a	L_P	D_{CC}	wt_{CC}	L_{CC}	λ_M
Value	2 cm	-2.5 cm	20 cm	0.3 mm	15 cm	8.47

The compliant tube and the compliant chambers (CC and CC_{RA}) were made of latex and constructed by the authors, with the mechanical properties in terms of compliance analysed in previous work [43].

In this test rig, the instrumentation consists of five bidirectional ultrasonic flowmeters: F1, F2, F3 (Sonoflow CO.55/190 V2.0, Sonotec, Germany) F4 and F5 (Sonoflow CO.55/100 V2.0, Sonotec, Germany) and five pressure meters: P1, P2, P3, P4 and P5 (TruWave, Edwards Lifescience, USA). The ultrasonic flowmeters have an accuracy of 2%, while the pressure meters have an accuracy of 1.5%. The flowmeters were used to measure instantaneous flow-rate Q_{IVC}, Q_{SVC}, Q_{TV}, Q_D and Q_R in the inferior vena cava, superior vena cava, tricuspid valve, drainage line and return line, respectively. The pressure meters were used to measure P_{IVC}, P_{SVC}, P_{RA}, P_D and P_R pressure in the inferior vena cava, superior vena cava, right atrium, drainage line and return line, respectively. A schematic of the test rig with instrumentation is shown in Figure 6.4. The direction of the arrows marks the positive flow direction criterion.

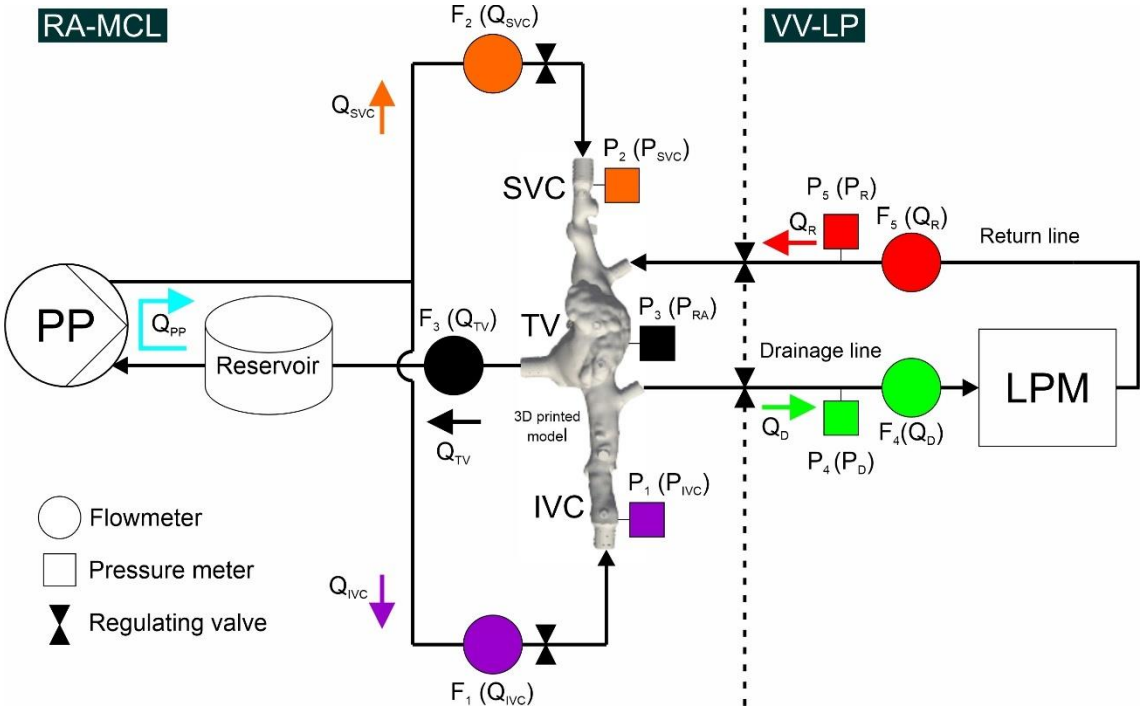

Figure 6.4. Schematic diagram of the complete loop with the different measuring instruments arranged in the circuit.

The design of the test rig allows the separation of the RA-MCL circuit from the VV-ECMO circuit and, thus, the recreation of the anatomical flow conditions in the physiological circuit.

Control and measurement systems

The control system from [50,52] was used to set the piston pump to reproduce a physiological flow profile (Q_{PP}) with great versatility in terms of heart rate and systolic volume. In this case, the flow profile was defined by seven interpolation points, as shown in Figure 6.5. Q_{PP} was calculated as the sum of flow to the inferior (Q_{IVC}) and superior (Q_{SVC}) vena cava. In particular, the flow profiles from venae cavae, evaluated in-vivo in [53], were used as a reference to calculate the interpolation points of Figure 6.5. A physiological cycle period of $T_C = 900$ ms was fixed for all tests.

The control system includes also real-time graphical display of sensor acquisitions and data logging configuration. The pressure and flow signals were acquired during thirty consecutive physiological cycles with a sampling period of 0.2 ms.

Point	1	2	3	4	5	6	7
Q [l min^{-1}]	0	16	6.7	10.6	0	-25	0
t / T_C	0	0.17	0.32	0.44	0.6	0.81	1

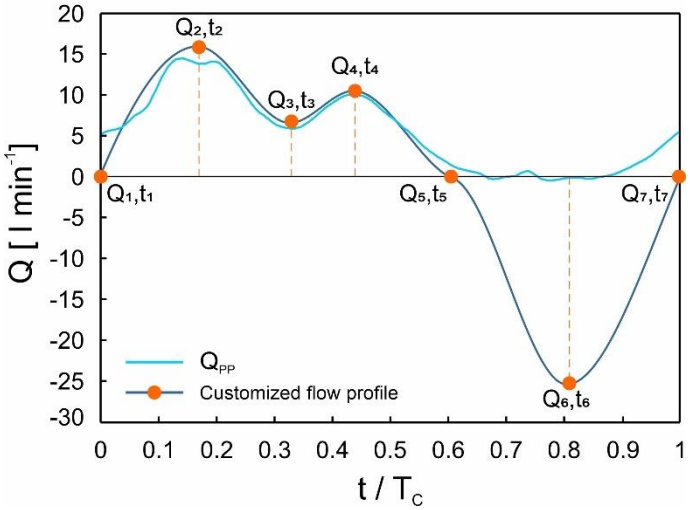

Figure 6.5. Parameterized flow through the piston pump (dark blue curve) and flow measured at the outlet of the piston pump in the cavae venae (light blue curve).

Concerning the Liebau pump, the operating cycle of the soft robot has two phases. In the first phase (pincher closed) compressed air enters the internal chamber of the soft robot, causing its wall to deform towards the compliant tube and compress it. This drives the fluid inside the compliant tube towards its ends. In the second phase (pincher open), the chamber is depressurised, and the soft robot regains its initial shape. The duty cycle (γ) is defined as the percentage of the operating cycle period in which the pincher is closed, compressing the compliant tube. The operating cycle control (OCC) of the Liebau pump allows to set the pinching frequency (f) and the duty cycle. [38,42,54].

Test plan

Three different tests were performed; test 1 evaluates the capability of the RA-MCL to reproduce the physiological cycle, test 2 evaluates the Liebau pump behavior without physiological cycle (PP switched off), and test 3 evaluates the Liebau pump performances with the physiological cycle (PP switched on).

Test 1 – To reproduce the physiological fluid dynamic condition of the RA, without any extracorporeal circulation device, the flows present in the venae cavae and tricuspid valve during the physiological cycle have been tuned in the RA-MCL circuit. To emulate the anatomical flow in the venae cavae, the flow split was regulated by imposing the flow as already described in the previous section (see Figure 6.5) and by

adjusting the regulation valves. To emulate the physiological flow in the tricuspid valve, the average flow profile observed in the work of [55] [Figure 6.7b] using MRI through the tricuspid valve in patients with some tricuspid valve regurgitation (reverse flow in TV) has been used as a reference. Tricuspid valve regurgitation has also been observed in volunteers without cardiovascular pathology [56]. The influence of the right atrium compliant chamber length (L_{CCRA}) on the flow through the tricuspid valve orifice will allow for adjusting the flow profile through it.

Test 2 - The Liebau pump tests without physiological cycle allows to analyse the the VV-LP behaviour if connected to RA-MCL in the absence of flow imposed by the piston pump. The effect of the length of the compliant chamber (L_{CC}) on the flow present in the VV-LP circuit has been studied. In particular, the flow was evaluated in terms of Q_D, Q_R and net flow (Q_{NET}), defined as the average of the instantaneous flowrate values during the test. All tests are carried out under stationary conditions. The dimensions and geometric parameters of the elements present in RA-MCL (tubing, CC_{RA}) were kept fixed during the tests. The VV-LP parameters including geometric parameters (Table 1) were modified from the baseline values for parametric studies. Operating parameters, duty cycle and the operating pressure, are also varied.

Test 3 - The Liebau pump with the physiological cycle allows to analyse the LPM behaviour under a scenario that simulates the hemodynamics in the right atrium of an ECMO patient. A sweep of pinching frequencies for different operating pressures (P_t) was imposed to specify the resonant frequency. At the resonant frequency, γ and P_t were varied to reach the maximum pump net flow. For each series of tests, geometric parameters of VV-LP, operating parameters (γ and P_t) and pinching frequency (*f*) were specified.

Results

Physiological cycle at RA-MCL

In the Figure 6.6, the temporal flow profiles in the venae cavae are shown. By parameterising the flow imposed by the piston pump and regulating the valves present in each of the venae cavae, it is possible to obtain flow rate profiles close to those determined

in vivo. As can be seen in Figure 6.6, the flow profiles obtained in the RA-MCL for the venae cavae can be considered representative of the physiological ones.

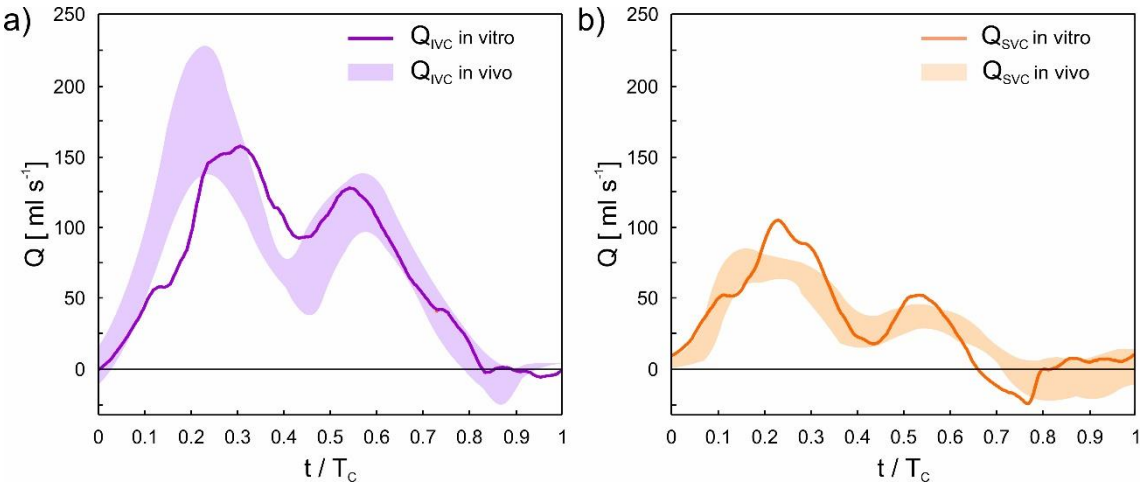

Figure 6.6. Flow profile in the (a) inferior (Q_{IVC}) and (b) superior (Q_{SVC}) vena cava during a physiological cycle, with *in vivo* flow ranges from [53].

The influence of the length of the compliant chamber of the RA (L_{CCRA}) on flow through the tricuspid valve orifice is shown in Figure 6.7a. It is possible to highlight that the L_{CCRA} increase induces a profile shape modification. For L_{CCRA} under 6.5 cm, a double peak behavior was encountered, which is in line with the physiological trend of Q_{TV}. For this reason, L_{CCRA}= 4.3 cm was established as the parameter to fit the physiological flow in the TV [Figure 6.7b]. The existing mismatch is within the physiological variability. The flow profile in the venae cavae was virtually unaffected with variations in L_{CCRA}.

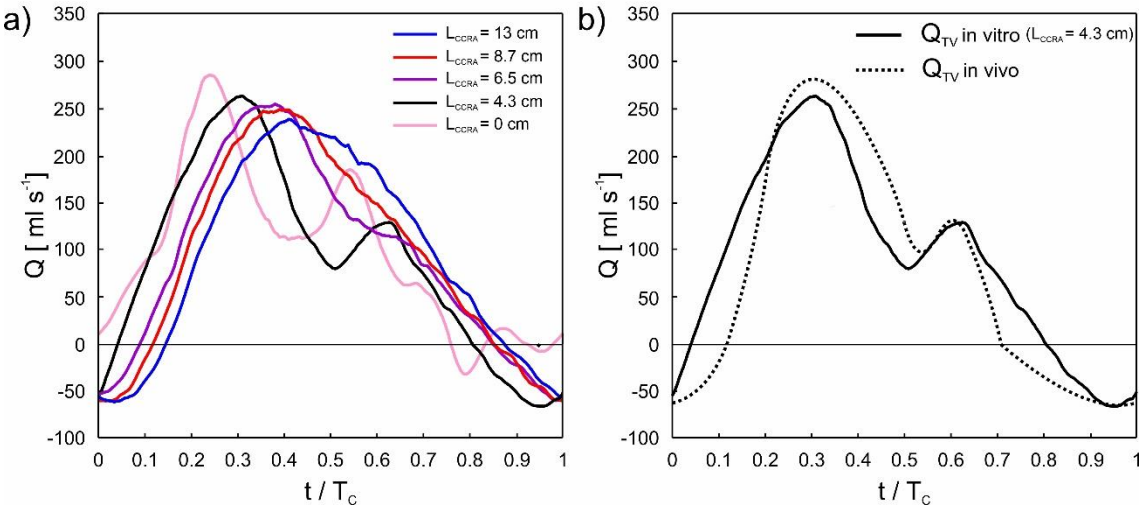

Figure 6.7. (a) Q_{TV} during a physiological cycle for different L_{CCRA} values and (b) comparison with *in vivo* data from [55] for L_{CCRA}= 4.3 cm.

The gauge pressures measured in the inferior vena cava P_{IVC}, superior vena cava P_{SVC} and right atrium P_{RA} during the physiological cycle are shown in Figure 6.8 for different L_{CCRA} values. The pressure oscillations could be due to pressure waves generated by the piston pump in combination with the model rigidity. As observed in the Q_{TV}, the damping effect of the L_{CCRA} was observed in the pressure waveforms. As L_{CCRA} gets larger, the pressure oscillations are, in fact, damped. In the absence of flow, the pressure at these points was 17 mmHg, determined by the height of the free surface of the fluid in the reservoir (23 cm).

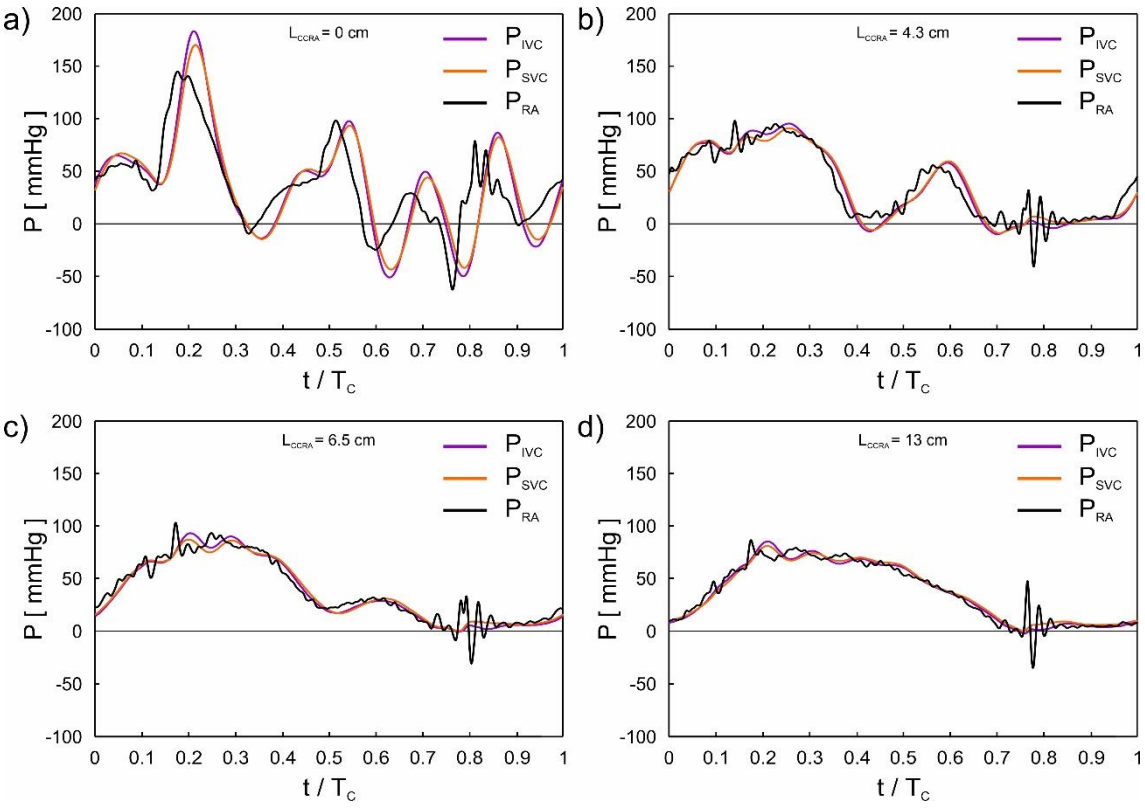

Figure 6.8. Pressure oscillation in the IVC, SVC and RA during a physiological cycle for (a) L_{CCRA}= 0 cm (b) L_{CCRA}= 4.3 cm (c) L_{CCRA}= 6.5 cm and (d) L_{CCRA}= 13 cm.

Liebau pump without physiological cycle

It should be noted, that in this experimental series the aim was not to obtain the maximum performance of the Liebau pump, but to analyse the influence of the length of the compliant chamber (L_{CC}) of the LPM on the flow evolution in VV-LP. The impact of L_{CC} on the resulting Q_{NET} and on Q_D - Q_R is represented in Figure 6.9. The test conditions were fixed to baseline geometric parameters for VV-LP, γ= 33%, P_t= 1.4 bar and f= 3 Hz.

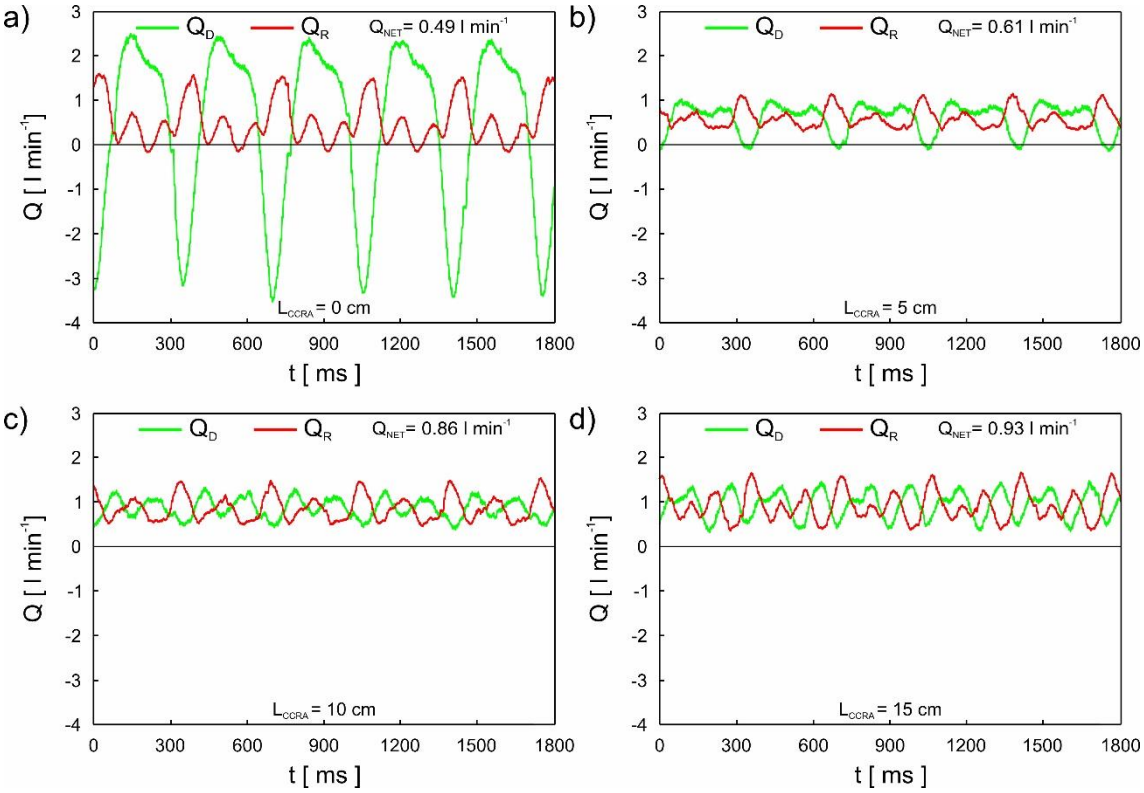

Figure 6.9. Analysis of the influence of L_{CC}. (a) L_{CC}= 0 cm, Q_{NET}= 0.49 l min^{-1}, (b) L_{CC}= 5 cm, Q_{NET}= 0.61 l min^{-1}, (c) L_{CC}= 10 cm, Q_{NET}= 0.86 l min^{-1} and (d) L_{CC}= 15 cm, Q_{NET}= 0.93 l min^{-1}.

The calculated Q_{NET} values show that as L_{CC} increases, the net flow also increases. On the other hand, if L_{CC} is too short, reverse flow appears in the drainage and return line [Figure 6.9a], or only in the drainage line [Figure 6.9b]. It is possible to observe that for L_{CC}= 15 cm no reverse flow was encountered in Q_R and grants the maximum observed Q_{NET}. Additionally, the increment of Q_{NET} with L_{CC} was 40% between 5 >L_{CC}> 10 cm, while 8% between 10 >L_{CC}> 15 cm. For this reason, L_{CC}= 15 cm was used for the subsequent tests.

Liebau pump with physiological cycle

Frequency sweep

The objective of these tests is to determine the resonant frequency, which maximizes the performance of the Liebau pump [38,57].

Figure 6.10 shows the relationship between pinching frequency (*f*) and net flow rate (Q_{NET}) by varying the operating pressure parameter (P_t). The test conditions were baseline geometric parameters at VV-LP, γ= 33%, P_t= 1.2, 1.6 and 2 bar. As previously

shown in [42], a higher operating pressure (P_t) translates into a higher closing speed of the soft robotic pincher when compressing the compliant tube. This, in turn, results in a higher instantaneous flow rate and, therefore, a higher kinetic energy difference between the drainage line and the return line. Thus, there is a higher net flow through VV-LP. The resonant frequency found is close to 4.5 Hz.

In Figure 6.10, it is also observed that the direction and magnitude of the net flow rate does not depend linearly on the pinching frequency, which is a characteristic of valveless pumping based on the Liebau effect [37,39].

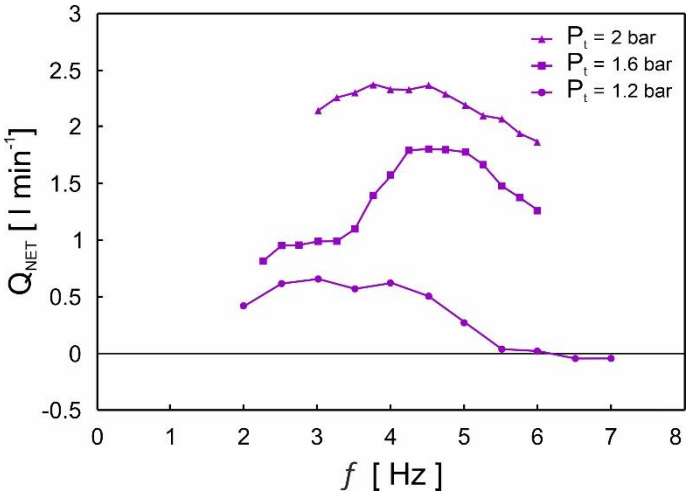

Figure 6.10. Analysis of the influence of P_t in Q_{NET} for different pinching frequencies sweeps.

Influence of the operating parameters at resonant frequency

The aim of this section is to find the operating conditions that maximize the Liebau pump performance. Figure 6.11 shows the influence of the operating parameters (P_t, γ) on the net flow rate for the resonant frequency assessed in the previous section. The ranges of variation of the operating parameters used, guarantee the correct functioning of the soft robotic pincher It is possible to observe that Q_{NET} is not influenced by P_t, if the pressure remains under a certain threshold, which depends on the γ value. Is interesting to highlight that Q_{NET} remains negligible for $\gamma = 10\%$, regardless of the imposed P_t. On the other hand, if the threshold is overcome, a direct proportionality exists between P_t and Q_{NET}. Additionally, Q_{NET} increases with γ maintain a fixed P_t value.

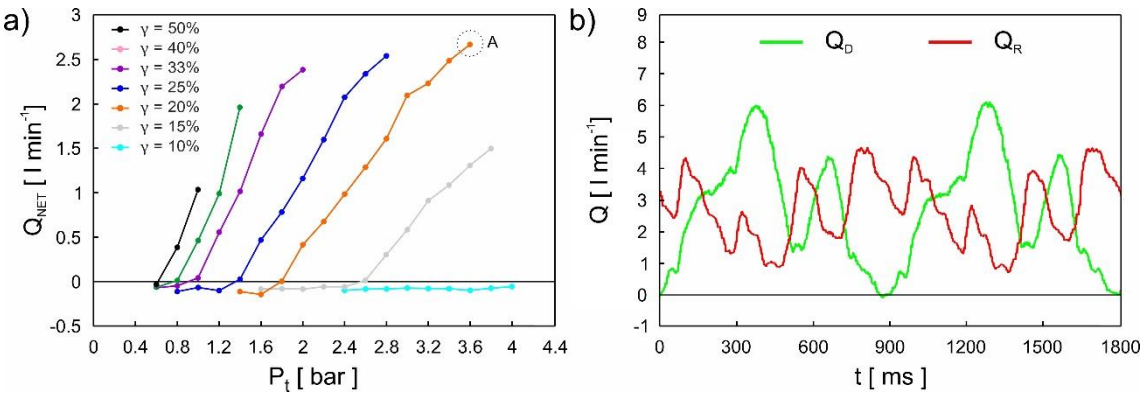

Figure 6.11. (a) Analysis of the influence of P_t and γ. (b) Evolution of the instantaneous flow rate in the drainage and return lines for the operating conditions of point A., (2 physiological cycles) Q_{NET}=2.7 l min^{-1}.

According to this, it can be seen that the maximum net flow rate (2.7 l min^{-1}) is obtained for the operating parameters γ= 20%, P_t= 3.6 bar (point A of Figure 6.11a). This value is within the range of use for low-flow ECMO (<3 l min^{-1}) [58] and in the paediatric range of patients up to 30 kilograms [22].

Figure 6.11b shows for point A indicated in Figure 6.11a the instantaneous flow rates Q_D and Q_R during two physiological cycles. It is possible to observe the pulsatility of both waveforms, with no reverse flow reported. The existence of pulsatile flow in the return line is an advance over the continuous flow centrifugal pumps currently used in extracorporeal circulation. The long-term absence of pulsatile flow is associated to several complications, from increased vascular stiffness [59] to reduced organ perfusion [27] and ischemic strokes [60]. Additionally, pulsatility promotes the movement of blood in the vessels, avoiding stagnant regions. A great advantage of this technology would be the possibility to adjust the frequency of the Liebau pump to allow the synchronization of its operating cycle with the physiological one, avoiding recirculation of oxygenated blood to the ECMO system, increasing the overall ECMO performance. [32–34]. This aspect would enhance the overall performance of ECMO operation and benefit the patient. Future work will be the finalization of the mock loop setup to obtain a more realistic ECMO environment by, for example, adding an oxygenator unit. In addition, we will explore the possibility of operating with ECMO without recirculation of oxygenated blood.

Conclusion

This work pioneers the feasibility and adoption of a valveless Liebau pump for ECMO, with various advantages for extracorporeal blood pumping in comparison with traditional pumping equipment. A right atrium mock circulatory loop emulating a veno-venous ECMO test rig is tested experimentally, substituting the traditional centrifugal pump for a soft-robotics Liebau pump developed by the authors. The influence of different geometric and configuration parameters of the proposed pump is discussed and optimum values for assistance during ECMO are found. The integration of such pump in the ECMO circuit is satisfactory, showing a flow assistance up to 2.7 L/min, lying in the range of pediatric ECMO and low blood flow range for adults. The Liebau pump approach was demonstrated to be a promising alternative to the veno-venous ECMO test rig, with the potential to achieve several advantages thanks to the flow pulsatility provided. In the future, the test rig will be improved to make it more similar to a real circuit by adding cannulae and an oxygenator.

Acknowledgments

The authors would like to thank the Junta de Castilla y León for funding this work as part of the program "Subvenciones del programa de apoyo a proyectos de investigación financiados por fondos FEDER," project number VA182P20.

AUTHORS DECLARATIONS

Conflict of interest

The authors declare that they have no conflicts to disclose.

Author Contributions

J. Anatol: Conceptualization, Data Curation, Investigation, Methodology, Validation, Visualization, Writing – Original Draft. **E. Vignali:** Methodology, Resources, Software, Writing – Original Draft. **E. Gasparotti:** Methodology, Resources, Software, Writing – Original Draft. **F. Castro-Ruiz:** Conceptualization, Methodology, Project administration, Visualization, Writing – Review & Editing. **M. Rubio:** Conceptualization, Validation, Writing – Original Draft. **C. Barrios-Collado:** Conceptualization, Validation, Writing – Original Draft. **J. Sierra-Pallares:** Conceptualization, Funding acquisition, Methodology, Supervision, Visualization,

Writing – Review & Editing. **S. Celi:** Conceptualization, Funding acquisition, Methodology, Project administration, Resources, Supervision, Visualization, Writing – Review & Editing.

Data Availability

The data that support the findings of this study are available from the corresponding author upon reasonable request.

Nomenclature

a	Width of the pinching region
CC	Compliant chamber
CC_{RA}	Compliant chamber of the right atrium
d	Inner diameter of flexible pipes
D	Inner diameter of rigid pipes
D_C	Inner diameter of the compliant tube
D_{CC}	Inner diameter of the compliant chamber
ECMO	Extracorporeal membrane oxigenation
ELSO	Extracorporeal Life Support Organization
f	Frequency
F1	Flowmeter in inferior vena cava
F2	Flowmeter in superior vena cava
F3	Flowmeter in tricuspid valve
F4	Flowmeter in drainage line
F5	Flowmeter in return line
IVC	Inferior vena cava
LPM	Liebau pump module
L_A	Length of the suction pipe

L_B Length of the intermediate pipe

L_C Length of the compliant tube

L_{CC} Length of the compliant chamber

L_{CCRA} Length of the compliant chamber of the right atrium

L_D Length of the drainage line

L_P Length between the compliant tube and pinching region symmetry planes

L_R Length of the return line

L_T Length of the extracorporeal circuit

L_1 Length between the flexible pipe of drainage line and the compliant tube symmetry plane

L_2 Length between the flexible pipe of return pipe and the compliant tube symmetry plane

MRI Magnetic resonance imaging

OCC Operating cycle control

P Pressure

PP Piston pump

PVC Polyvinyl chloride

P_D Pressure meter in drainage line

P_{IVC} Pressure in inferior vena cava

P_{RA} Pressure meter in right atrium

P_R Pressure meter in return line

P_{SVC} Pressure meter in superior vena cava

P_t Operating pressure

P1 Pressure meter in inferior vena cava

P2 Pressure meter in superior vena cava

P3 Pressure meter in tricuspid valve

P4 Pressure meter in drainage line

P5 Pressure meter in return line

References

[1] S. Torregrosa *et al.,* «Oxigenación de membrana extracorpórea para soporte cardíaco o respiratorio en adultos», *1134-0096*, vol. 16, no. 2, pp. 163–177, 2009.

[2] M. J. Chakaramakkil y C. Sivathasan, «ECMO and Short-term Support for Cardiogenic Shock in Heart Failure», *Current cardiology reports*, vol. 20, no. 10, p. 87, 2018.

[3] G. MacLaren, A. Combes y R. H. Bartlett, «Contemporary extracorporeal membrane oxygenation for adult respiratory failure: life support in the new era», *Intensive care medicine*, vol. 38, no. 2, pp. 210–220, 2012.

[4] D. Abrams, A. Combes y D. Brodie, «Extracorporeal membrane oxygenation in cardiopulmonary disease in adults», *Journal of the American College of Cardiology*, vol. 63, no. 25 Pt A, pp. 2769–2778, 2014.

[2] A. Combes *et al.,* «Outcomes and long-term quality-of-life of patients supported by extracorporeal membrane oxygenation for refractory cardiogenic shock», *Critical care medicine*, vol. 36, no. 5, pp. 1404–1411, 2008.

[6] L. Dangers *et al.,* «Extracorporeal Membrane Oxygenation for Acute Decompensated Heart Failure», *Critical care medicine*, vol. 45, no. 8, pp. 1359–1366, 2017.

[7] Zapol, W. M. et al., «Extracorporeal Membrane Oxygenation in Severe Acute Respiratory Failure», JAMA, vol 242, no. 20, pp 2195-2196, 1979.

[8] Hill J. Donald *et al.,* «Prolonged Extracorporeal Oxygenation for Acute Post-Traumatic Respiratory Failure (Shock-Lung Syndrome)», 1972.

[9] E. Khoshbin *et al.,* «Poly-methyl pentene oxygenators have improved gas exchange capability and reduced transfusion requirements in adult extracorporeal membrane oxygenation», *ASAIO journal (American Society for Artificial Internal Organs: 1992)*, vol. 51, no. 3, pp. 281–287, 2005.

[10] A. Maslach-Hubbard y S. L. Bratton, «Extracorporeal membrane oxygenation for pediatric respiratory failure: History, development and current status», *World journal of critical care medicine*, vol. 2, no. 4, pp. 29–39, 2013.

[11] J. Javidfar *et al.,* «Use of bicaval dual-lumen catheter for adult venovenous extracorporeal membrane oxygenation», The *Annals of thoracic surgery*, vol. 91, no. 6, 1763-8; discussion 1769, 2011.

[12] D. Wang *et al.,* «Wang-Zwische double lumen cannula-toward a percutaneous and ambulatory paracorporeal artificial lung», *ASAIO journal (American Society for Artificial Internal Organs: 1992)*, vol. 54, no. 6, pp. 606–611, 2008.

[13] C. M. Sauer, D. D. Yuh y P. Bonde, «Extracorporeal membrane oxygenation use has increased by 433% in adults in the United States from 2006 to 2011», *ASAIO journal (American Society for Artificial Internal Organs: 1992)*, vol. 61, no. 1, pp. 31–36, 2015.

[14] S. Allen *et al.,* «A review of the fundamental principles and evidence base in the use of extracorporeal membrane oxygenation (ECMO) in critically ill adult patients», Journal *of intensive care medicine*, vol. 26, no. 1, pp. 13–26, 2011.

[15] M. L. Paden, S. A. Conrad, P. T. Rycus y R. R. Thiagarajan, «Extracorporeal Life Support Organization Registry Report 2012», ASAIO *journal (American Society for Artificial Internal Organs: 1992)*, vol. 59, no. 3, pp. 202–210, 2013.

[16] J. E. Tonna *et al.,* «Management of Adult Patients Supported with Venovenous Extracorporeal Membrane Oxygenation (VV ECMO): Guideline from the Extracorporeal Life Support Organization (ELSO)» , *ASAIO journal (American Society for Artificial Internal Organs: 1992)*, vol. 67, no. 6, pp. 601–610, 2021.

[17] E. Vignali, E. Gasparotti, D. Haxhiademi y S. Celi, «Fluid dynamic model for extracorporeal membrane oxygenation support and perfusion in cardiogenic shock», *Physics of Fluids*, vol. 35, no. 11, 2023.

[18] A. F. Stephens *et al.,* «Comparison of Circulatory Unloading Techniques for Venoarterial Extracorporeal Membrane Oxygenatio», *ASAIO journal (American Society for Artificial Internal Organs: 1992)*, vol. 67, no. 6, pp. 623–631, 2021.

[19] D. Han *et al.,* «Computational fluid dynamics analysis and experimental hemolytic performance of three clinical centrifugal blood pumps: Revolution, Rotaflow and CentriMag», *Medicine in novel technology and devices*, vol. 15, 2022.

[20] R. C. d. F. Chaves *et al.,* «Oxigenação por membrana extracorpórea: revisão da literatura», *Revista Brasileira de terapia intensiva*, vol. 31, no. 3, pp. 410–424, 2019.

[21] S. Robinson y G. Peek, «The role of ECMO in neonatal & paediatric patients», *Paediatrics and Child Health*, vol. 25, no. 5, pp. 222–227, 2015.

[22] C. Maratta *et al.,* «Extracorporeal Life Support Organization (ELSO): 2020 Pediatric Respiratory ELSO Guideline», *ASAIO journal (American Society for Artificial Internal Organs: 1992)*, vol. 66, no. 9, pp. 975–979, 2020.

[23] K. J. Rehder *et al.,* «Technological advances in extracorporeal membrane oxygenation for respiratory failure», *Expert review of respiratory medicine*, vol. 6, no. 4, pp. 377–384, 2012.

[24] L. Lequier, S. B. Horton, D. M. McMullan y R. H. Bartlett, «Extracorporeal membrane oxygenation circuitry», *Pediatric critical care medicine: a journal of the Society of Critical Care Medicine and the World Federation of Pediatric Intensive and Critical Care Societies*, vol. 14, no. 5 Suppl 1, S7-12, 2013.

[25] Y. S. Moon, S. Ohtsubo, M. R. Gomez, J. K. Moon y Y. Nose, «Comparison of Centrifugal and Roller Pump Hemolysis Rates at Low Flow», *Artificial organs*, vol. 20, no. 5, pp. 579–581, 1996.

[26] D. B. Tulman *et al.,* «Veno-venous ECMO: a synopsis of nine key potential challenges, considerations, and controversies», *BMC anesthesiology*, vol. 14, p. 65, 2014.

[27] J. van der Merwe, E. Paul y F. L. Rosenfeldt, «Early Gastrointestinal Complications from Ventricular Assist Devices is Increased by Non-Pulsatile Flow», *Heart, lung & circulation*, vol. 29, no. 2, pp. 295–300, 2020.

[28] B. Illum *et al.,* «Evaluation, Treatment, and Impact of Neurologic Injury in Adult Patients on Extracorporeal Membrane Oxygenation: a Review», *Current*

treatment options in neurology, vol. 23, no. 5, p. 15, 2021. doi: 10.1007/s11940-021-00671-7

[29] C. O'Brien, J. Monteagudo, C. Schad, E. Cheung y W. Middlesworth, «Centrifugal pumps and hemolysis in pediatric extracorporeal membrane oxygenation (ECMO) patients: An analysis of Extracorporeal Life Support Organization (ELSO) registry data», *Journal of pediatric surgery*, vol. 52, no. 6, pp. 975–978, 2017.

[30] C. A. Figueroa Villalba *et al.,* «Thrombosis in Extracorporeal Membrane Oxygenation (ECMO) Circuits», *ASAIO journal (American Society for Artificial Internal Organs: 1992)*, vol. 68, no. 8, pp. 1083–1092, 2022.

[31] S. M. Hastings, D. N. Ku, S. Wagoner, K. O. Maher y S. Deshpande, «Sources of Circuit Thrombosis in Pediatric Extracorporeal Membrane Oxygenation», *ASAIO journal (American Society for Artificial Internal Organs: 1992)*, vol. 63, no. 1, pp. 86–92, 2017.

[32] S. A. Conrad y D. Wang, «Evaluation of Recirculation During Venovenous Extracorporeal Membrane Oxygenation Using Computational Fluid Dynamics Incorporating Fluid-Structure Interaction», *ASAIO journal (American Society for Artificial Internal Organs: 1992)*, vol. 67, no. 8, pp. 943–953, 2021.

[33] A. Xie, T. D. Yan y P. Forrest, «Recirculation in venovenous extracorporeal membrane oxygenation», *Journal of critical care*, vol. 36, pp. 107–110, 2016.

[34] D. Abrams, M. Bacchetta y D. Brodie, «Recirculation in venovenous extracorporeal membrane oxygenation», *ASAIO journal (American Society for Artificial Internal Organs: 1992)*, vol. 61, no. 2, pp. 115–121, 2015.

[35] G. Liebau, «ber ein ventilloses Pumpprinzip», *Naturwissenschaften*, vol. 41, no. 14, p. 327, 1954.

[36] A. Aghilinejad, B. Rogers, H. Geng y N. M. Pahlevan, «On the longitudinal wave pumping in fluid-filled compliant tubes», *Physics of Fluids*, vol. 35, no. 9, 2023.

[37] S. Timmermann y J. T. Ottesen, «Novel characteristics of valveless pumping», *Physics of Fluids*, vol. 21, no. 5, 2009.

[38] C. Manopoulos *et al.,* «Net flow generation in closed-loop valveless pumping», *Proceedings of the Institution of Mechanical Engineers, Part C: Journal of Mechanical Engineering Science*, vol. 234, no. 11, pp. 2126–2142, 2020.

[39] A. I. Hickerson y M. Gharib, «On the resonance of a pliant tube as a mechanism for valveless pumping», *J. Fluid Mech.*, vol. 555, p. 141, 2006.

[40] N. Sarvazyan, «Building Valveless Impedance Pumps from Biological Components: Progress and Challenges», *Frontiers in physiology*, vol. 12, p. 770906, 2021.

[41] J. Anatol *et al.,* «An assessment of the suitability of a Liebau pump in biomedical applications», *Physics of Fluids*, vol. 36, no. 1, 2024.

[42] J. Anatol *et al.,* «Experimental characterization of an asymmetric valveless pump based on soft robotics technology», *Physics of Fluids*, vol. 35, no. 6, 2023.

[43] J. Anatol *et al.,* «Experimental study of an asymmetric valveless pump to elucidate insights into strategies for pediatric extravascular flow augmentation», *Scientific reports*, vol. 12, no. 1, p. 22165, 2022.

[44] I. Avrahami y M. Gharib, «Computational studies of resonance wave pumping in compliant tubes», *J. Fluid Mech.*, vol. 608, pp. 139–160, 2008.

[45] C.-Y. Wen y H.-T. Chang, «Design and Characterization of Valveless Impedance Pumps», *J. mech.*, vol. 25, no. 4, pp. 345–354, 2009.

[46] T. Kenner, «Biological Asymmetry and Cardiovascular Blood Transport», *Cardiovascular Engineering*, vol. 4, no. 2, pp. 209–218, 2004.

[47] T. T. Bringley *et al.,* «An experimental investigation and a simple model of a valveless pump», *Physics of Fluids*, vol. 20, no. 3, 2008.

[48] S. Celi *et al.,* «3D Printing in Modern Cardiology», *Current pharmaceutical design*, vol. 27, no. 16, pp. 1918–1930, 2021.

[49] B. M. Fanni *et al.,* «An integrated in-vitro and in-silico workflow to study the pulmonary bifurcation hemodynamics», *Computers & Fluids*, vol. 260, p. 105912, 2023.

[50] E. Vignali *et al.,* «High-Versatility Left Ventricle Pump and Aortic Mock Circulatory Loop Development for Patient-Specific Hemodynamic In Vitro Analysis», *ASAIO journal (American Society for Artificial Internal Organs: 1992)*, vol. 68, no. 10, pp. 1272–1281, 2022.

[51] C. Banfi *et al.,* «Veno-venous extracorporeal membrane oxygenation: cannulation techniques», *Journal of thoracic disease*, vol. 8, no. 12, pp. 3762–3773, 2016.

[52] F. Bardi, E. Gasparotti, E. Vignali, S. Avril y S. Celi, «A Hybrid Mock Circulatory Loop for Fluid Dynamic Characterization of 3D Anatomical Phantoms», *IEEE transactions on bio-medical engineering*, vol. 70, no. 5, pp. 1651–1661, 2023.

[53] M. Markl *et al.,* «Time-resolved three-dimensional magnetic resonance velocity mapping of cardiovascular flow paths in volunteers and patients with Fontan circulation», *European journal of cardio-thoracic surgery: official journal of the European Association for Cardio-thoracic Surgery*, vol. 39, no. 2, pp. 206–212, 2011.

[54] A. I. Hickerson, D. Rinderknecht y M. Gharib, «Experimental study of the behavior of a valveless impedance pump», *Exp Fluids*, vol. 38, no. 4, pp. 534–540, 2005.

[55] J. J. M. Westenberg *et al.,* «Mitral valve and tricuspid valve blood flow: accurate quantification with 3D velocity-encoded MR imaging with retrospective valve tracking», *Radiology*, vol. 249, no. 3, pp. 792–800, 2008.

[56] H. W. Kayser, B. C. Stoel, E. E. van der Wall, R. J. van der Geest y A. de Roos, «MR velocity mapping of tricuspid flow: correction for through-plane motion», *Journal of magnetic resonance imaging: JMRI*, vol. 7, no. 4, pp. 669–673, 1997.

[57] S. Takagi y T. Saijo, «Study of a Piston Pump without Valves: 1st Report, On a Pipe-capacity-system with a T-junction», *Bulletin of JSME*, vol. 26, no. 218, pp. 1366–1372, 1983.

[58] K. Lehle *et al.,* «Flow dynamics of different adult ECMO systems: a clinical evaluation», *Artificial organs*, vol. 38, no. 5, pp. 391–398, 2014.

[59] A. C. Patel *et al.,* «Dynamic Changes in Aortic Vascular Stiffness in Patients Bridged to Transplant with Continuous-Flow Left Ventricular Assist Devices», *JACC. Heart failure*, vol. 5, no. 6, pp. 449–459, 2017.

[60] J. Z. Willey *et al.,* «Outcomes after stroke complicating left ventricular assist device», *The Journal of heart and lung transplantation: the official publication of the International Society for Heart Transplantation*, vol. 35, no. 8, pp. 1003–1009, 2016.